Sensors & Transducers, Vol. 249, Issue 2, February 2021, pp. 1-8

www.sensorsportal.com

Sensors & Transducers

Published by IFSA Publishing, S. L., 2021
http://www.sensorsportal.com

Applying Neural Nets on Sensor Noise to Identify CT Scanner Manufacturers

[1] Markus GERLOFSMA, [1, 2, *] Milan PETKOVIC, [2] Peter van LIESDONK and [1] Vlado MENKOVSKI

[1] Eindhoven University of Technology, Eindhoven, The Netherlands
[2] Royal Philips Research Laboratories, Eindhoven, The Netherlands
[*] E-mail: m.petkovic@tue.nl

Received: 10 October 2020 /Accepted: 10 December 2020 /Published: 28 February 2021

Abstract: The acquisition of Computed Tomography (CT) images has shown to be affected by the scanning device which acquires the image. Specifically, the same subject, scanned by a variety of CT devices, holds different properties depending on the device which acquired the image. This variance consequently has an impact on the medical analysis of the images. Therefore, the ability to determine the acquiring CT device based on the produced CT images may lead to improved diagnoses. In addition, knowledge of the CT device may furthermore provide a means to ensure verification of provenance without the necessity to rely on potentially corrupt or missing DICOM metadata. In this work, we apply a Convolutional Neural Network (CNN) to classify 4 manufacturers of CT scanners, based on the CT images which their devices generate. We apply our experiments on a large, publicly available dataset, and additionally apply previous classification techniques on the same dataset. With an accuracy of up to 93.6 %, our approach significantly outperforms existing work.

Keywords: CT scanners, CT Device Manufacturers, CT Image Classification, Convolutional Neural Networks, Sensor Noise.

1. Introduction

Computed Tomography (CT) has become a vital asset in medical imaging. CT scans are volumetric images which are acquired by capturing a multitude of slices via x-ray beams. These slices are captured at consecutive angles and together form the entirety of a CT volume. Fig. 1 depicts examples of such slices. Once captured, the complete CT images are then predominantly stored as a file in the DICOM imaging format [1]. In addition to the image data itself, this storage format also provides additional metadata about the parameters of the acquisition process of the image and the properties of the capturing CT device. One such device property is the manufacturer of the scanning device.

Such information may be exceptionally valuable as, for example, the estimation of lung density using CT images has shown to vary among CT scanner devices from different device manufacturers, which consequently affects the diagnosis of Emphysema [2], [3]. As such, knowledge of certain DICOM metadata, such as the device manufacturer of the scanner, may improve medical diagnoses themselves.

However, the DICOM metadata which contains this information is predominantly implemented without any security checks and requires only a few mandatory fields to produce a valid file. This leniency causes the metadata to be often incomplete and susceptible to modifications, which may discourage medical professionals to confidently act on the available data. Although the DICOM standard

facilitates additional controls which provide data integrity, these measures are predominantly not implemented to ensure a painless data exchange between parties, such as hospitals.

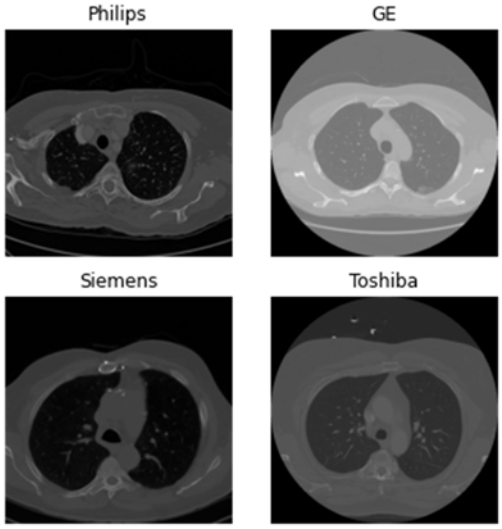

Fig 1. Example of CT slices from the LIDC-IDRI dataset.

To reduce the dependency on DICOM metadata, yet still exploit the benefit of the underlying data, the authors of [4] sought to identify a specific CT scanner device, exclusively based on the image data of a CT scan. The authors extracted the Sensor Pattern Noise (SPN) from the images to obtain distinct device fingerprints for a series of CT scanner devices and used image correlation to perform device identification based on these fingerprints. In addition to precise device identification, these noise patterns may also be leveraged to determine the integrity of the images themselves, which furthermore make them an attractive security control to e.g. detect image tampering [5].

Despite the initial success, the work in [4] exclusively applied an elemental classification approach based on image correlation, which consequently provides an opportunity for potential improvement. Convolutional Neural Networks (CNN) [6] have shown excellent performance for image classification and representation learning in several domains, including applications on medical images, including CT scans [7]. Therefore, they may also prove to be an excellent tool to learn precise device fingerprints and classify CT device manufacturers based on CT images.

As such, different from the related work, we apply a CNN to classify 4 CT manufacturers based on the CT images produced by their respective CT scanners. In our paper we demonstrate the remarkable capability of neural networks to perform CT scanner classification based on CT images as well as sensor noise. We furthermore provide novel insights and show how the extraction of distinct noise patterns has a significantly varying effect on the classification. Finally, we demonstrate the importance of sensible data processing for a task such as CT device classification.

2. Related Work

To attribute images to specific devices, in the seminal work of [8], the authors leveraged the Photo Response Non-Uniformity noise (PRNU) present in the Sensor Pattern Noise (SPN) of pictures taken by photo cameras to attribute images to specific camera models. To extract the noise component of an image, the approach uses a denoising filter based on the work of [9]. This filter is applied on several images from the same, known camera model, and are subsequently averaged to obtain a reference pattern for a specific camera model. This reference pattern then serves as the fingerprint for the device, which enables attribution of future images.

This same denoising and classification procedure has been applied in [4] to identify CT scanners. Therein, the authors consider a total of 3 scanners from 2 manufacturers to perform CT scanner device identification based on the CT images produced by the corresponding scanner. The same authors have furthermore improved this experimental setup by adding an additional correction step during noise extraction [10] and experimented with computing the noise pattern along different dimensions of the original CT image [11].

Aside from specific CT device identification, other works aim to classify a group of devices instead [12], [13]. These works rely on alternative pre-processing steps, supplemented with an SVM [14] to perform the final classification. In [12], an alternative denoising technique is applied to account for the unique image acquisition and reconstruction process of CT images. The authors conducted their experiments on images containing a variety of anatomical objects to classify a total of 17 scanner models produced by 4 manufacturers. Differently, the work in [13] distinguished 3 CT scanner manufacturers by performing a quantitative analysis based on the density distribution of Hounsfield Unit (HU) values within the CT images. The authors fit an SVM on the found distributions and achieve an accuracy of 91.1 %.

One limiting factor we discovered in the related works is that these works are exclusively based on smaller, private datasets, which poses a challenge in making a direct and fair comparison of the achieved results. Furthermore, previous works which applied noise extraction as a preprocessing step, have not performed their classification technique on unprocessed CT images. For this reason, to our knowledge, there also does not yet exist a baseline for the classification of device manufacturers based on unprocessed CT images. This absence of a baseline limits the ability to make confident assertions about the effect of noise extraction on the classification performance.

Different from the related work, this is the first work to perform the classification on both unprocessed CT images and extracted noise patterns, which will indicate the potential benefit of noise extraction when performing device classification. In addition, this work is the first to apply a deep learning method to classify CT scanner manufacturers based on the acquired CT images. Finally, we use a larger, publicly available dataset, containing images from a wider array of devices to provide a better indication for the generalizability of CT scanner classification.

3. Approach

Within our experiments, we first and foremost aim to evaluate the effectiveness of neural nets in identifying CT device manufacturers based on the sensor noise present within a CT image. However, in order to draw sensible conclusions, we also seek to establish a baseline for our experiments. For this reason, we first reproduce and apply the classification technique initially performed in [4], but on a significantly larger dataset than the initial work. We apply this approach on the unprocessed CT slices, as well as on the extracted sensor noise patterns.

Then, for the classification using neural networks, we construct and train two convolutional neural networks (CNN) [6] to classify the slices of CT images. Here, the setup is again twofold. One CNN is trained and tested on unprocessed slices, while the second network is trained to classify the extracted sensor noise of the CT slices.

3.1. Noise Extraction Algorithm

The sensor noise components (Fig. 2) from a CT slice is extracted by applying the approach proposed in [8]. Although this approach has been initially proposed for the identification of photo cameras, the technique has also shown success in identifying CT scanners by the images which they produce [4], [10], [11].

To denoise a slice, a denoising filter *F* is applied. The denoised image is subtracted from the original slice to obtain the desired noise component *w*:

$$\mathrm{w} = \mathrm{s} - F(s \qquad (1)$$

The denoising filter *F* is the same as applied in [8], [9]. Specifically, the work applies a Wiener filter in the wavelet domain, which is applied in two stages as follows. First, the local variance of the image within the wavelet domain is estimated. Then, in the second stage, the estimated variance is applied in a Wiener filter to obtain the denoised image. These two stages are performed using the steps described below:

1) The fourth-level wavelet decomposition is calculated for the slice.

2) For each level, the three high frequency-bands are used for further processing. These are the vertical, horizontal and diagonal sub-bands, respectively.

3) For each wavelet coefficient in the sub-bands, the local variance $\hat{\sigma}^2(i,j)$ is estimated within a $W \times W$ square neighbourhood, for $W \in \{3,5,7,9\}$. The minimum of these 4 variances is chosen as the final estimate for the image variance:

$$\hat{\sigma}_W^2(i,j) = \max\left(0, \frac{1}{W^2} \sum_{(i,j)\in N} h^2(i,j)\, \hat{\sigma}_0^2\right) \qquad (2)$$

$$\hat{\sigma}^2(\mathrm{i},\mathrm{j}) = \min\left(\hat{\sigma}_3^2(i,j),\ \hat{\sigma}_5^2(i,j),\ \hat{\sigma}_7^2(i,j),\ \hat{\sigma}_9^2(i,j)\right), \qquad (3)$$

where $(i,j) \in \mathrm{J}$ denotes the index set for decomposition level J, and $\hat{\sigma}_0^2$ is a manually tuned parameter which has been set to $\hat{\sigma}_0^2 = 5$ to follow the original work [8].

4) After the variance estimation, the Wiener filter is applied to obtain the denoised wavelet coefficients:

$$X_{den}(i,j) = X(i,j) \frac{\hat{\sigma}^2(i,j)}{\hat{\sigma}^2(i,j) + \hat{\sigma}_0^2} \qquad (4)$$

5) The above steps 2−4 are repeated for each wavelet sub-band, on each level of the decomposition.

6) The final, denoised image *F(s)* is then obtained by applying the inverse wavelet transform.

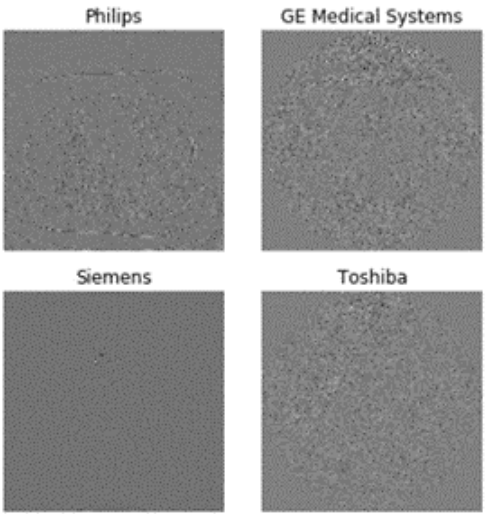

Fig. 2. Example of extracted noise patterns from several CT slices.

3.2. Reference Pattern and Correlation

The baseline classification approach, based on correlation with a reference pattern, is performed by applying the same technique as [4]. This approach is performed in two stages. First, a reference pattern is computed for each class of CT scanners by averaging a random selection of slices from a particular class of scanners. The original process, illustrated in Fig. 3, applies this technique exclusively on the extracted noise patterns. However, since we additionally evaluate this approach on the unprocessed slices, we

skip the noise extraction step in one instance of our experiments. The classification stage, illustrated by Fig. 4, then performs the classification by calculating the correlation of a CT slice, or its extracted noise component *w*, with each of the computed reference patterns *RP*:

$$\mathrm{corr}(\mathrm{s},\mathrm{RP}) = \frac{(s-\bar{s})\left(RP-\overline{RP}\right)}{||s-\bar{s}||\,||RP-\overline{RP}||} \qquad (5)$$

The resulting correlation with a reference pattern indicates the likelihood that the image originates from the same device. Although the original work [4] accomplished this by establishing a certain threshold for the correlation value, we base the decision on the pattern that exhibits the highest correlation.

3.3. Data Split

When performing classification on the 2D slices of a CT image, one may consider two approaches to split the data into their respective training and test sets. The first approach, presented in Fig. 5, accumulates the 2D CT slices from the dataset, and subsequently divides them into separate sets for training and testing. Differently, the second approach, illustrated by Fig. 6, accumulates the slices per volume and subsequently divides the slices of entire volumes into the respective sets.

To our knowledge, the related works [4], [10], [11], [12] have solely considered the first approach. As such, no volume is excluded during the training phase and computation of the reference patterns. However, this first approach may lead to optimistic results as the test set is likely affected by undesired relationships between individual slices which have been generated during the same scanning session of a patient. Specifically, successive, neighboring slices are generally captured within a distance of just 1-3 millimeters. This small difference between the captured slices causes these images to depict nearly identical content. For this reason, the first approach to split the data, shown in Fig. 5, assigns nearly identical slices into both training and test set, and therefore may lead to skewed classification performance.

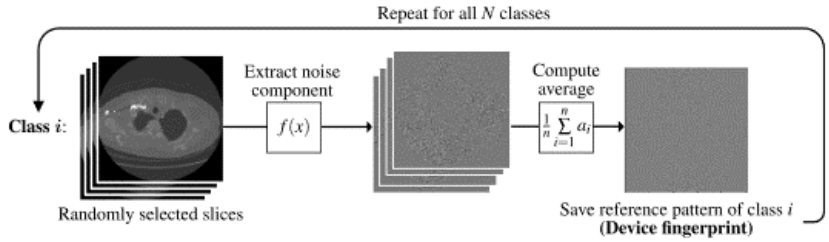

Fig. 3. Creation of reference patterns for a certain amount of devices, given a set of slices from known devices.

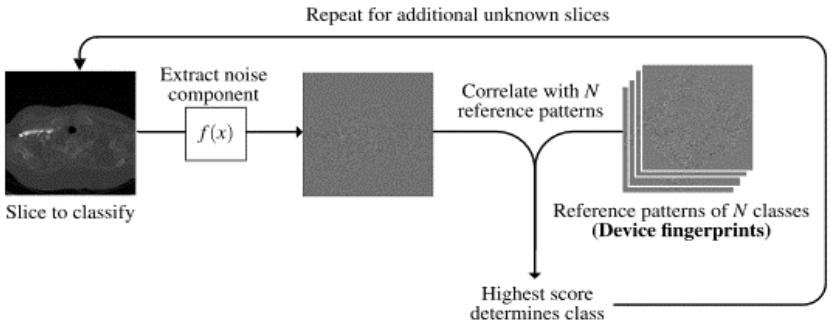

Fig. 4. The process to determine the class of unknown slices, given a precomputed set of reference patterns.

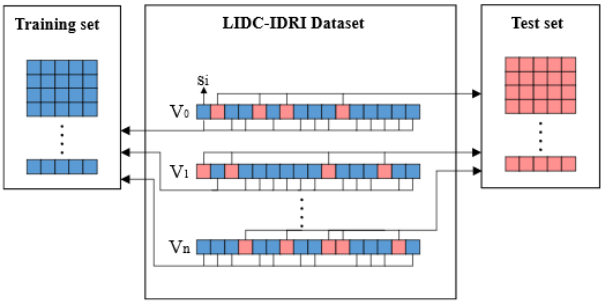

Fig. 5. A split based on individual CT slices. Neighbouring slices may end in either split.

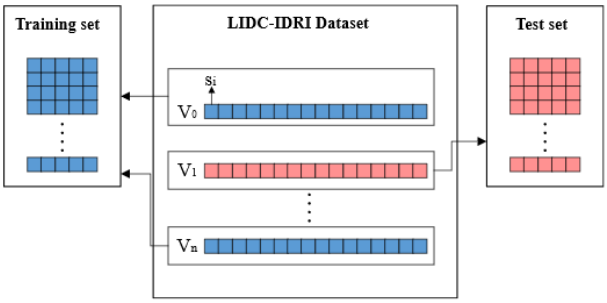

Fig. 6. A split based on CT Volumes. This type of split will keep several potential relationships among slices within a single side of the split.

For this reason, in our experiments, we primarily consider data splits based on the second, volume-based approach illustrated in Fig. 6. However, we also perform the alternative, first approach a single time to highlight the significance of a sensible data split.

4. Dataset

All experiments in our work are performed on samples from the anonymized and publicly accessible collection of CT imagery from the Lung Image Database Consortium and Image Database Resource Initiative (LIDC-IDRI) [15]. This dataset contains a total of 1,018 CT volumes, amounting to a total of 244,527 slices. The volumes in this dataset are represented by a total of 4 manufacturers: Philips, GE Healthcare, Siemens, and Toshiba. These manufacturers consequently form the 4 classes for the experiments. Table 1 illustrates the representation of each class within the LIDC-IDRI dataset. The CT scans in this dataset are stored in the 'Digital Imaging and Communications in Medicine' (DICOM) file format[1] which, besides the image data and device manufacturer. In this work, we make use of the metadata within the DICOM format to determine the true label (device manufacturer) of the CT slices.

Table 1. CT volume representation within the LIDC-IDRI dataset.

Manufacturer	No. of Volumes
Philips	75
Siemens	206
GE healthcare	671
Toshiba	70

It is important to note that, besides the manufacturer of a CT scanner, the specific content of the image may be affected by additional circumstances. For example, the images contained within the dataset have been captured by a variety of CT scanner models. The dataset contains images from a total of 15 specific CT scanner models. The specific make of a CT scanner model may also impact the overall performance of a certain class, when for example, a certain model is produced and calibrated differently from other models by the same manufacturer.

However, given the number of images within the dataset, as well as our experimental setup, we hope to eliminate as many potential biases as possible.

5. Experimental Setup

In each experiment, the manufacturer classification is performed on the slices from the LIDC-IDRI [15] dataset. To account for the class imbalance in the LIDC-IDRI dataset, the classes have been balanced by under sampling over-represented classes. As such, the final dataset used in the experiments contained 6,000 slices per class. To extract the noise patterns (Section 3.1) from the CT images, the implementation from [5] has been applied, who have kindly published their source code[2].

To perform the experiments based on the reference pattern and correlation metric (Section 3.2), we continue to primarily follow the work of [4]. Specifically, the reference patterns for the manufacturers are computed using the average of 120 slices per class. However, differently from the initial work, we explicitly split the data as visualized in Fig. 6. As such, slices from volumes which are used to calculate the reference pattern, are entirely separated from the volumes that are classified during the test phase. During classification, each slice from the test set will be compared to each of the reference patterns by calculating the correlation (Equation (5)), where the highest correlation value determines the class.

For the classification using a CNN, a simple, common architecture for image classification has been applied. Specifically, this architecture contained three convolutional layers, with a number of 8, 16 and

[1] https://www.dicomlibrary.com/dicom/

[2] Available at: http://dde.binghamton.edu/download/camerafingerprint/

32 3×3 filters, respectively, with each convolutional layer being followed by a Batch normalization layer [16] and ReLU activation function. The first two convolutional blocks are furthermore followed by a 2×2 max pooling layer, while the last block contains an additional dropout layer to avoid overfitting. Finally, to increase the computational speed, input dimensions have been reduced from the original 512×512 to 299×299. An overview of the architecture is presented in Fig. 7. This architecture performed well on all tasks and has been applied for both networks which classify based on noise patterns and unprocessed slices, respectively. The networks were trained for 10 epochs, on batches of size 128.

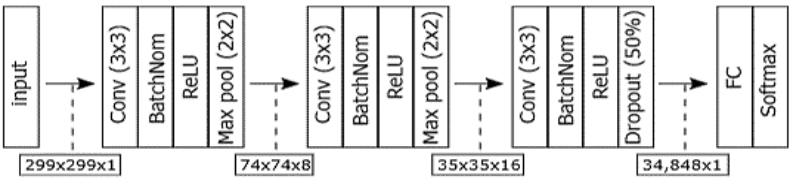

Fig. 7. The CNN architecture used for the classification of CT scanners.

6. Results

6.1. Reference Pattern and Correlation

Table 2 presents the classification accuracies on extracted noise patterns using the reference pattern and correlation metric, initially applied in the work of [4]. The results show that slices from Toshiba and General Electric are classified perfectly, while CT slices from both Siemens and Philips are classified significantly worse. It is also peculiar that Philips and Siemens are most often misclassified amongst each other, which may indicate that these devices share certain software or hardware components or share similarities in the physical acquisition process of the images which consequently affect the device fingerprint.

For the classification on the original, unprocessed slices, the result presented in Table 3 shows that predictions are significantly more distributed compared to the accuracies on noise patterns.

Table 2. Classification accuracy by correlation on extracted noise patterns of CT images.

	Philips	**Siemens**	**GE**	**Toshiba**
Philips	**29.55 %**	33.9 %	22.4 %	14.15 %
Siemens	37.78 %	**35.92 %**	14.58 %	11.72 %
GE	-	-	**100 %**	-
Toshiba	-	-	-	**100 %**
Average	**66.4 % accuracy**			

Table 3. Classification accuracy by correlation on unprocessed CT images.

	Philips	**Siemens**	**GE**	**Toshiba**
Philips	**77.85 %**	22.15 %	-	-
Siemens	29.66 %	**53.91 %**	13.43 %	**3.00 %**
GE	-	-	**76.5 %**	**23.5 %**
Toshiba	-	-	40.97 %	**59.03 %**
Average	**66.8 % accuracy**			

However, the overall accuracy remains similar to the previous result, with a slight increase to 66.8 %, up from the previous 66.4 %. Moreover, predictions for General Electric and Toshiba devices have become split amongst each other and are classified significantly worse. However, Philips and Siemens devices are predicted more accurately on the original images. Interestingly, prediction mistakes for a certain class often fall into just one single, other class.

Nevertheless, the relatively low accuracy on either type of input image indicates that classification based on image correlation with a reference pattern may be insufficient to make accurate predictions on extensive datasets.

6.2. Classification with Neural Networks

As it can be seen in Table 5, the CNN reaches significantly better results and achieves up to 93.6 % classification accuracy on the noise patterns of CT slices. This is a significant improvement over the correlation-based experiments which achieved a maximum accuracy of 66.8 %. In addition, the neural network also outperforms the work of [13] which performed classification on just 3 manufacturers. Moreover, the deep learning classifier reached 1.1 % higher accuracy on the classification of noise patterns as opposed to the classification on original, unprocessed CT slices, presented in Table 4. This result suggests that the extraction of device fingerprints does not interfere with the capability of the neural network to learn its own features. Interestingly, the misclassifications shown in Table 4 also continue to support the apparent similarity between Siemens and Philips devices already highlighted in Section 6.1.

6.3. Effect of Data split

Finally, the CNN has also been evaluated on the naive train/test split in which data is solely separated based on individual slices (Fig. 5). Table 6 shows that this approach indeed significantly favors the classification. The classifier reaches an accuracy of

99.8 % which even outperforms the much smaller setting presented in [4]. This result consequently confirms the hypothesis that the classification of CT scanner manufacturers still requires careful consideration when the data is split into separate sets.

Table 4. Classification accuracy on unprocessed CT images with a neural network.

	Philips	**Siemens**	**GE**	**Toshiba**
Philips	**72.63 %**	27.37 %	-	-
Siemens	1.27 %	**98.73 %**	-	-
GE	-	-	**100 %**	-
Toshiba	-	-	-	**100 %**
Average	**92.5 % accuracy**			

Table 5. Classification accuracy on extracted noise patterns of CT images with a neural network.

	Philips	**Siemens**	**GE**	**Toshiba**
Philips	**98.55 %**	1.45 %	-	-
Siemens	8.40 %	**77.82 %**	-	**13.78 %**
GE	-	-	**100 %**	-
Toshiba	-	-	-	**100 %**
Average	**93.6 % accuracy**			

Table 6. Classification of CT images using a slice-based data split.

	Philips	**Siemens**	**GE**	**Toshiba**
Philips	**99.57 %**	0.43 %	-	-
Siemens	-	**100 %**	-	-
GE	-	0.14 %	**99.64 %**	0.21 %
Toshiba	-	-	-	**100 %**
Average	**99.8 % accuracy**			

7. Conclusions

In this paper, we presented several experiments aimed to classify CT scanner manufacturers based on individual, 2D CT image slices. We evaluated an existing approach, based on the work of [4], on a larger dataset and under stricter conditions. Next, in our approach, we evaluated a CNN on the same task. For both approaches, we performed an additional pre-processing step which extracts the noise component from a CT slice to obtain a representation of the underlying device fingerprint. We compared this pre-processing step to the classification based on the original, unprocessed images. Finally, we showed that this classification task requires careful consideration when splitting the data in respective train and test set.

The results have shown that the classification approach based on reference patterns is not suitable for larger datasets, which naturally carry more variation. In addition, the extraction of the SPN had no significant impact on the performance of this approach. Conversely, the CNN showed outstanding accuracy, and with an accuracy of up to 93.6 %, even out-performed existing work. The classification on the SPN-fingerprint performed only slightly better than the unprocessed images. However, the gained performance is only marginal and may become less significant in fully optimized networks.

8. Discussion and Future Work

The results of the experiments have shown that CNNs are an effective method to classify scanner devices based on CT imagery. Nevertheless, this work primarily serves as a first step towards scanner classification based on neural nets. As such, the methods used in this work may still be optimized. The neural networks applied in the experiments are based on existing architectures and setups, with slight modifications to suit the dimensions and the amount of data. As such, there is still ample opportunity to improve the existing classifiers based on additional domain expertise. In addition to the network optimization, the extracted noise pattern may also be substantially optimized. The current noise pattern to establish the fingerprint was originally intended for ordinary photo cameras yet has also shown applicability for CT scanners. However, in [12], improvements have already been made by applying more sophisticated device fingerprint based on the reconstruction algorithm of CT scanners. In addition, denoising of CT images is an extensively explored topic, and existing methods in this field may also benefit the extraction of more accurate device fingerprints.

Acknowledgements

The work presented in this paper is an extension of the publication featured in the conference proceedings of the international Conference on Advances in Signal Processing and Artificial Intelligence (ASPAI' 2020) [17]. Furthermore, this work is funded by the EC Horizon 2020 research and innovation programme under grant agreement No 780495 (BigMedilytics).

References

[1]. W. D. Bidgood Jr, S. C. Horii, F. W. Prior, D. E. Van Syckle, Understanding and using DICOM, the data interchange standard for biomedical imaging, *Journal of the American Medical Informatics Association*, Vol. 4, Issue 3, 1997, pp. 199-212.

[2]. R. Yuan, J. R. Mayo, J. C. Hogg, P. D. Par´e, A. M. McWilliams, S. Lam, H. O. Coxson, The effects of radiation dose and CT manufacturer on measurements of lung densitometry, *Chest*, Vol. 132, Issue 2, 2007, pp. 617–623.

[3]. B. C. Stoel, M. E. Bakker, J. Stolk, A. Dirksen, R. A. Stockley, E. Piit-ulainen, E. W. Russi, J. H. Reiber, Comparison of the sensitivities of 5 different computed tomography scanners for the assessment of the progression of pulmonary emphysema: a phantom study, *Investigative Radiology*, Vol. 39, Issue 1, 2004, pp. 1–7.

[4]. A. Kharboutly, W. Puech, G. Subsol, D. Hoa, CT-scanner identification based on sensor noise analysis, in *Proceedings of the 5th European Workshop on Visual Information Processing (EUVIP)*, 2014, pp. 1–5.
[5]. M. Chen, J. Fridrich, M. Goljan, J. Lukâs, Determining image origin and integrity using sensor noise, *IEEE Transactions on Information Forensics and Security*, Vol. 3, Issue 1, 2008, pp. 74–90.
[6]. Y. LeCun, Y. Bengio, *et al*., Convolutional networks for images, speech, and time series, *The Handbook of Brain Theory and Neural Networks*, Vol. 3361, Issue 10, 1995, p. 1995.
[7]. J. Kuruvilla, K. Gunavathi, Lung cancer classification using neural networks for CT images, *Computer Methods and Programs in Biomedicine*, Vol. 113, Issue 1, 2014, pp. 202-209.
[8]. J. Lukâs, J. Fridrich, M. Goljan, Digital camera identification from sensor pattern noise, *IEEE Transactions on Information Forensics and Security*, Vol. 1, Issue 2, 2006, pp. 205–214.
[9]. M. K. Mihcak, I. Kozintsev, K. Ramchandran, Spatially adaptive statistical modeling of wavelet image coefficients and its application to denoising, in *Proceedings of the IEEE International Conference on Acoustics, Speech, and Signal Processing, (ICASSP'99)* (Cat. No. 99CH36258), Vol. 6, 1999, pp. 3253–3256.
[10]. A. Kharboutly, W. Puech, G. Subsol, D. Hoa, Improving sensor noise analysis for ct-scanner identification, in *Proceedings of the IEEE 23rd European Signal Processing Conference (EUSIPCO)*, 2015, pp. 2411–2415.
[11]. A. Kharboutly, W. Puech, G. Subsol, D. Hoa, Advanced sensor noise analysis for CT-scanner identification from its 3D images, in *Proceedings of the IEEE International Conference on Image Processing Theory, Tools and Applications (IPTA)*, 2015, pp. 325–330.
[12]. Y. Duan, D. Bouslimi, G. Yang, H. Shu, G. Coatrieux, Computed tomography image origin identification based on original sensor pattern noise and 3D image reconstruction algorithm footprints, *IEEE Journal of Biomedical and Health Informatics*, Vol. 21, Issue 4, 2017, pp. 1039–1048.
[13]. S.-B. Lee, E.-J. Jeong, Y. Son, D.-J. Kim, Classification of computed tomography scanner manufacturer using support vector machine, in *Proceedings of the IEEE 5th International Winter Conference on Brain-Computer Interface (BCI)*, 2017, pp. 85–87.
[14]. C. J. Burges, A tutorial on support vector machines for pattern recognition, *Data Mining and Knowledge Discovery*, Vol. 2, Issue 2, 1998, pp. 121–167.
[15]. S. G. Armato III, G. McLennan, L. Bidaut, M. F. McNitt-Gray, C. R. Meyer, A. P. Reeves, L. P. Clarke, *et al*., Data from LIDC-IDRI. The cancer imaging archive, 2015. [Online]. Available: http://doi.org/10.7937/K9/TCIA.2015.LO9QL9SX
[16]. S. Ioffe, C. Szegedy, Batch normalization: Accelerating deep network training by reducing internal covariate shift, *arXiv preprint arXiv:1502.03167*v3, 2015.
[17]. M. Gerlofsma, M. Petkovic, P. Van Liesdonk, V. Menkovski, CT Scanner Classification with Neural Nets and Sensor Noise, in *Proceedings of the 2nd International Conference on Advances in Signal Processing and Artificial Intelligence (ASPAI'2020)*, Berlin, Germany, 18-20 November 2020, pp. 154-160.